Seismotectonic implications of strike–slip earthquakes in the Darjiling–Sikkim Himalaya

Malay Mukul[1,*], Sridevi Jade[2], Kutubuddin Ansari[1] and Abdul Matin[3]

[1]Department of Earth Sciences, Indian Institute of Technology Bombay, Powai, Mumbai 400 076, India
[2]CSIR-4PI, Formerly CSIR-CMMACS, Wind Tunnel Road, Bangalore 560 037, India
[3]Department of Geology, University of Calcutta, 35 Ballygunge Circular Road, Kolkata 700 019, India

The Darjiling–Sikkim Himalaya (DSH) is located over the Dharan–Gorubathan salient–recess pair and moderate thrust and strike–slip earthquake occur here. The hypocentres cluster not only near the location of the Main Himalayan Thrust (MHT) or the basal decollement of the Himalayan wedge, but also well above and below it. The epicentres cluster over the mapped location of the Lesser Himalayan Duplex (LHD), suggesting that both MHT and LHD are active structures in DSH. The earthquakes below MHT can be related to transverse strike–slip faulting in DSH associated with salient–recess transition on both flanks of the Dharan salient. The 18 September 2011 (*Mw* 6.9) strike–slip event suggests that the western flank of the Dharan salient is also likely to contain an active transverse strike–slip fault like the Gish Transverse Fault (GTF) on its eastern flank. High-precision Global Positioning System measurements (1997–2006) indicate that a maximum of ~4 mm/year convergence is being accommodated in the Tista Half-Window or LHD west of the surface trace of GTF and DSH is locked south of 27°N both east and west of GTF about 10 km north of the Himalayan mountain front. About 3–4 mm/year sinistral strike–slip is postulated on GTF north of 27°N. Dislocation based forward modelling using two thrust dislocations with oblique slip and a sinistral strike–slip dislocation generated velocities that were closest to the measured back-slip velocity field in DSH.

Keywords: Darjiling–Sikkim Himalaya, dislocation modelling, Global Positioning System, Gish Transverse Fault, recess, salient, seismicity.

Introduction

THE Indian plate collided with the Eurasian plate along a large-scale (in thousands of kilometres), frontal, arc-shaped Himalayan boundary[1–3]. However, smaller-scale sinuosity (in hundreds of kilometres) of the Himalayan mountain belt exists both in the Himalayan front as well as its hinterland (Figure 1). The sinuosity of the Himalayan front has been traditionally recognized in the western Himalaya as salients and recesses (e.g. Dehradun recess/re-entrant, Nahan salient and Kangra recess/re-entrant[4]; Figure 1) and more recently, in the eastern Himalaya as well (e.g. Dharan salient, Gorubathan recess; Figure 1)[5] and (Sarpang re-entrant)[6]. The salient–recess transitions are typically recognized to be lateral or oblique ramps[7,8] or tear faults[5,9]. Salients are typically associated with a mountain front defined by frontal imbricate faults (e.g. Nahan salient[4], Dharan salient[5,10]). Recesses, on the other hand, may be open to the foreland (e.g. Gorubathan or Sarpang[6] recesses in the eastern Himalaya) or may be forming intermontane, longitudinal valleys or Duns (e.g. Dehradun and Kangra recesses in the northwestern Himalaya; Figure 1) characterized by a frontal topographic high formed as a result of fault-related folding associated with a single thrust fault[4,11] (the Main Frontal Thrust (MFT) in the Dehradun and Kangra recesses). The Dun-type recess is not open to the foreland and sediments carried by the rivers that drain the recess are typically deposited in the Dun before being carried out into the foreland. Therefore, Himalayan salients, recesses and associated transitional structures have implications on the variation of the deformation kinematics along the length of the Himalayan arc over space and time.

The geometry of the Himalayan collision boundary is wedge-shaped (Figure 2); the base of this wedge is defined by a north-dipping decollement named the Main Himalayan Thrust (MHT)[12,13]. Several east-west trending and south-vergent, thrust faults such as the Main Central Thrust (MCT), Ramgarh Thrust (RT) and Main Boundary Thrust (MBT) sole (or meet at a very low angle[16,17]) with MHT[14,15]; the near-surface expression of MHT is MFT. The Himalayan wedge is defined as the region between the Indus-Tsangpo (locally named Zangbo) suture to the north and the Indo-Gangetic Himalayan foreland to the south. However, there is a conspicuous lack of data on the hinterland geometry of this wedge. The INDEPTH DSS work[13] is the only constraint that is available on the hinterland geometry of the Himalayan wedge and was carried out north of the Darjiling–Sikkim Himalayan (DSH) region that lies between the Nepal–India border to the west and the Bhutan Himalaya to the east[16]. This implies that the Darjiling–Sikkim–Tibet (DaSiT) Himalayan wedge is the most appropriate region to explore the first-order kinematic behaviour of the active Himalayan

*For correspondence. (e-mail: malaymukul@iitb.ac.in)

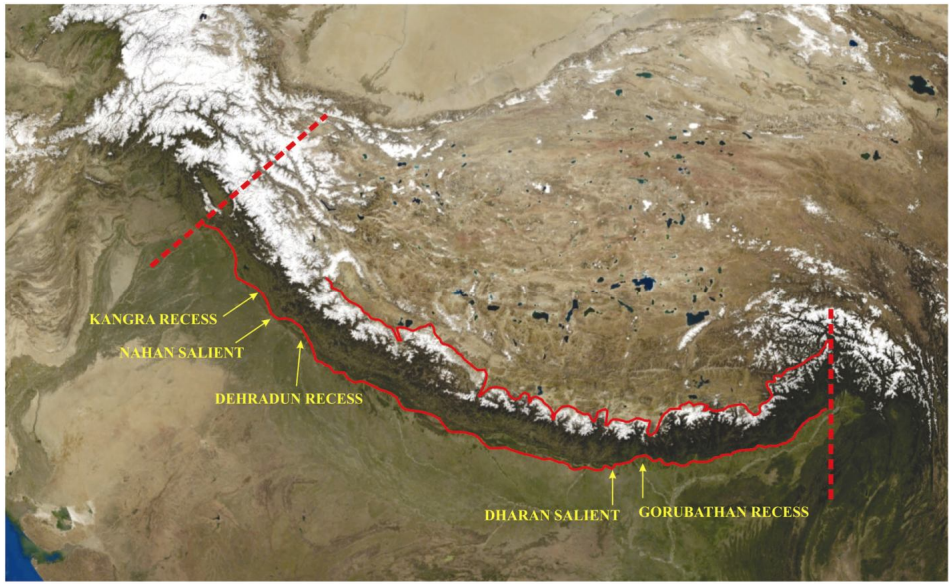

Figure 1. The Himalayan arc has a sinuous front at hundreds of kilometres scale even though it has been recognized as a perfect arc at larger scales[1]. The sinuosity is reflected in the formation of salients and recesses that are separated by transition zones such as active transverse tear faults. Sinuosity exists in the mountain front as well as in the hinterland as evident in the figure (Landsat-7 image from http://himalayamountains.com).

wedge[5,10]; this wedge is characterized by two 'dominant' structures[18] that are most likely to have built taper (defined as the sum of the basement dip and the topographic slopes angles of the wedge) in the wedge and driven the wedge forward into the foreland. First, the Kangmar Anticline[10,13,19], which is a crustal-scale, fault-bend fold associated with a crustal-scale ramp in the MHT near the Indus-Zangbo suture (Figure 2). Second, the Lesser Himalayan Duplex (LHD; Figure 2) that has been recognized as a prominent structure involving the Daling, Buxa and the Gondwana units through much of the lesser Himalaya in the DaSiT wedge[20,21]. The Kangmar Anticline was the 'dominant' structure that was responsible for driving the DaSiT Himalayan fold-thrust belt till ~10 Ma (ref. 5) and the emplacement of the RT and MCT sheets. The LHD has probably been responsible for driving the thrust belt into the foreland subsequently and the emplacement of the MBT and MFT thrust sheets[5].

This article discusses the seismotectonics of DSH in the light of modern concepts on the kinematics of fold-and-thrust belt deformation, published seismic data, high precision Global Positioning System (GPS) geodetic data collected in the area between 1997 and 2006, and dislocation modelling of the measured GPS velocities.

Seismicity of the Himalaya

The overall seismicity patterns in the Himalaya have been well established for decades[22], wherein the bulk of the Himalaya (with the exception of DSH) has been dominated by thrust earthquakes. Typically, the clustering of epicentres has been recognized to occur between the surface traces of MCT and MBT[23–26] and has been typically attributed to activity along MHT[23–25]. However, better constrained earthquake hypocentres (for example, figure 12 in ref. 25) indicate that all the seismicity cannot be located merely on an active MHT and there is activity within the Himalayan wedge above MHT between the surface traces of MBT and MCT. In the Garhwal and Kumaon Himalaya, balanced cross-sections[14,25] revealed the presence of LHD between the surface traces of MBT and MCT. This seems to indicate that LHD may be a seismically active structure in the Himalaya. This trend in seismicity seems to continue into Nepal and Sikkim Himalaya[23,27]. However, along-strike variation, the distribution of epicentres is also evident[23]. For example, the entire Himalayan wedge appears to be seismically active in eastern Nepal, whereas in the neighbouring Sikkim Himalaya, there appears to be little or no seismicity north of the MCT surface trace[23–27]. Again, in west-central Nepal, the entire Himalayan wedge seems to be seismically quiet[23]. These patterns in seismicity in Himalaya suggest that: (1) The Himalayan wedge is seismically active prominently between the surface traces of MBT and MCT, probably indicating that LHD is active in addition to MHT; (2) Lateral variations in the seismicity point to along-strike variations in active tectonics and seismicity in the Himalayan wedge and the need to identify uniformly deforming segments in a systematic manner.

Seismicity in DSH

Great earthquakes have not been recorded in the recent or historic past from the DaSiT wedge. Given this, it has been postulated that a great earthquake of magnitude > 7

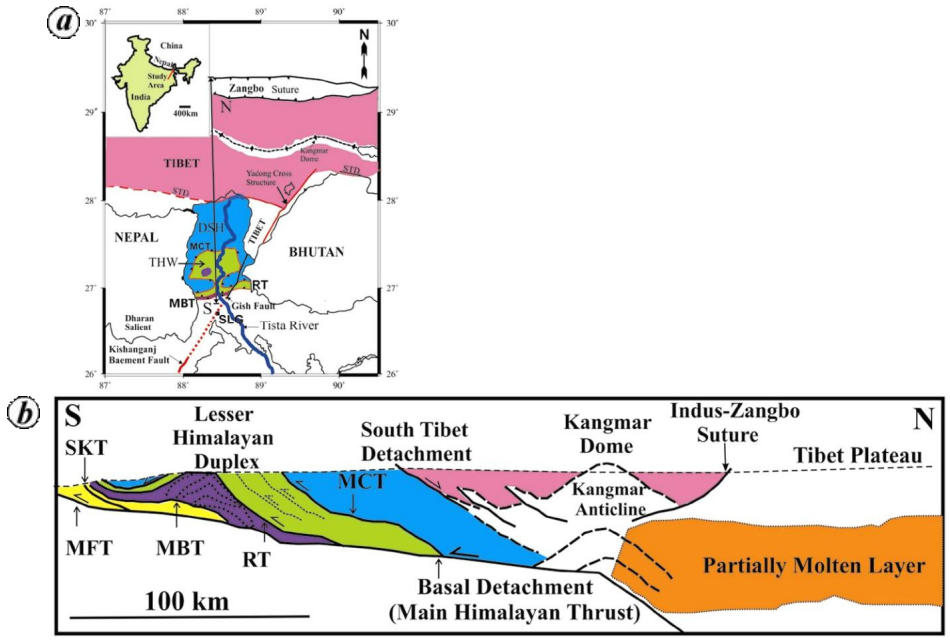

Figure 2. (*a*) Plan and (*b*) sectional view of the Darjiling–Sikkim–Tibet Himalayan wedge[5,10,13]. The wedge has two 'dominant' structures that probably drove the thrust belt towards south. DSH, Darjiling–Sikkim Himalaya; SKT, South Kalijhora Thrust; MCT, Main Central Thrust; RT, Ramgarh Thrust; MBT, Main Boundary Thrust; MFT, Main Frontal Thrust; THW, Tista Half Window; STD, South Tibet Detachment; SLG, Siliguri.

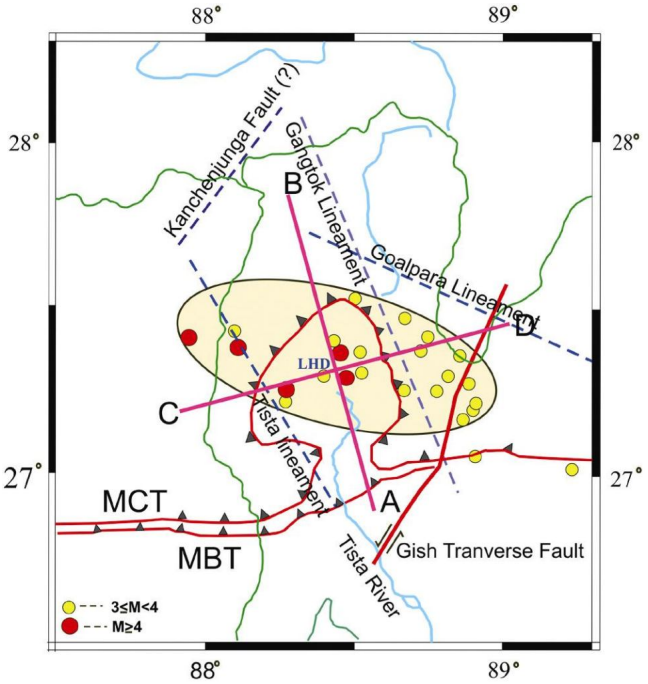

Figure 3. Distribution of seismicity in DSH[34,35]. Moderate earthquake distribution is shown as colour-coded circles. The micro-seismicity shows an oval distribution centred around the Lesser Himalayan Duplex (LHD) which indicates that LHD might be an active structure and causing the earthquakes. *AB* and *CD* are cross-sections along which earthquake distributions are shown in Figure 5.

is imminent in DSH[28]. The absence of recorded great earthquakes in the DaSiT wedge also indicates that the wedge is currently sub-critical[5,29]. The observed seismicity in DSH is dominated by frequent moderate earthquakes (DSH area in Figures 2 *a* and 3). The India Meteorological Department (IMD) network recorded 15 moderate earthquakes (> 4.5) in the region during 1982–1992 (ref. 30). A felt earthquake of $M = 5.0$ was also recorded in the region during a microearthquake survey (December 1992–April 1993) along with four earthquakes of magnitude ~4.0 (ref. 30). Subsequent microearthquake surveys carried out in the region during December 1994–March 1995 (ref. 31) and March–June 2000 (ref. 32) did not yield any earthquakes above magnitude 4.0. A strong motion array setup during 1999–2002 (ref. 33) recorded 12 moderate (> 5) earthquakes. Again, between October 2004 and February 2010, nine events with magnitude greater than or equal to 4, with 5.3 being the maximum magnitude, were observed in DSH[34]. Also, extensive seismological monitoring was carried out[26] in DSH during 2007–2009 with a well-defined seismic network consisting of 18 seismograph stations. A total of 756 earthquakes ($M < 6.0$) were recorded between 2007 and 2009. The strongest concentration of epicentres was found to occur between the surface traces of MBT and MCT. The Darjiling–Sikkim area, therefore, appears to be releasing accumulated strain through frequent moderate and microearthquakes (Figure 3). The seismicity in general appears to be diffused but located between MCT and MBT and lat. 27°N and 27.5°N (refs 24, 26, 30–35) indicating that THW records majority of the earthquakes in the area. In contrast, eastern Nepal records moderate and microearthquakes along the entire length of the Himalayan wedge[23,27].

Table 1. Focal mechanisms of the moderate earthquakes in the DSH

Reference	Date	Latitude (°N)	Longitude (°E)	Depth (km)	Magnitude	Focal mechanism	Strike	Dip	Rake	Fault plane solution
1[62]	19/11/1980	27.39	88.75	17	6.2	Strike–slip	209	51	–2	
2[62]	26/03/2005	28.08	87.95	69.6	4.7	Strike–slip	200	89	28	
3[62]	14/02/2006	27.22	88.64	19.2	5.3	Thrust	287	27	127	
4[62]	20/05/2007	27.23	88.56	13.6	4.9	Strike–slip	204	58	–4	
5[27]	12/2/2001	27.34	88.31	22	4.8	Strike–slip	182	16	–	
6[52,62]	12/01/1965	27.40	87.84	23	6.1	Strike–slip	090	75	90	
7[57,62]	05/04/1982	27.38	88.83	9.0	5.1	Strike–slip	206	48	–30	
8[57,63]	18/09/2011	27.74	88.11	35	6.9	Strike–slip	220	78	0	

Focal mechanisms of earthquakes

Focal mechanisms of the moderate earthquakes in the DSH indicate both thrust and strike–slip earthquakes (Table 1; Figure 4). Prominent thrust earthquakes in the region include the 14 February 2006 Sikkim earthquake of magnitude 5.3 (*Mw*)[35–37]. However, moderate strike–slip earthquakes abound in the region[22,27,35,37]. Significant strike–slip earthquakes include the 19 November 1980 Sikkim earthquake of *Mb* 6.2 (ref. 38), the 12 February 2001 earthquake of *Mw* 4.8, the 20 May 2007 earthquake of *Mw* 4.9 (ref. 27) and the 18 September 2011, *Mw* 6.9 earthquake close to the Nepal–Sikkim border[39–41]. This indicates that both strike–slip and thrust seismotectonics are operational in DSH. The challenges are to figure out the seismogenic structures in the DaSiT wedge and work out the kinematics of deformation in these structures. North of the Himalaya in the Tibet Plateau, seismicity seems to be dominated by extensional or normal earthquakes primarily along N–S normal faults[22].

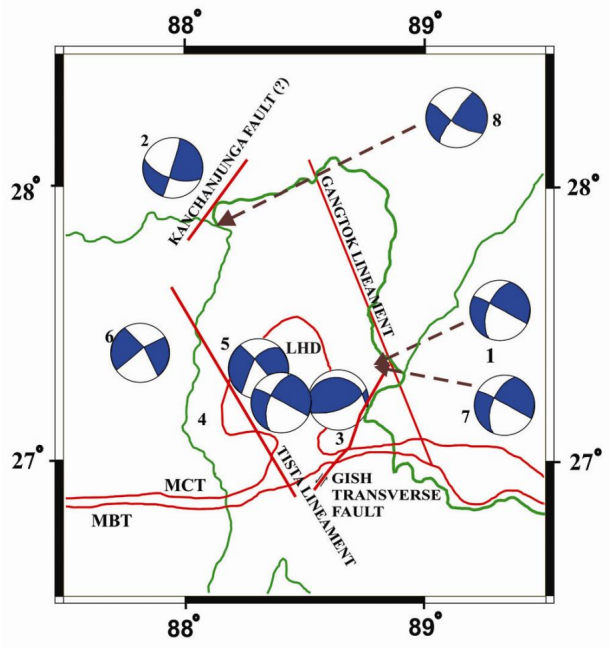

Figure 4. Map showing the main focal mechanisms seen in DSH (data available in Table 1). Both moderate thrust and strike–slip earthquakes are seen in the DaSiT wedge, which points to the fact that both thrusting and strike–slip faulting are active in DSH.

Thrust seismotectonics

Thrust earthquakes have been traditionally designated to MHT in the Himalayas[23,27,28]. Additionally, MCT has been recognized as the seismogenic fault responsible for thrust earthquakes[32,33,42] in DSH. However, the seismicity in DSH is predominantly confined to the THW (Figure 3) with a large concentration at shallow (0–20 km) depths[26] (figure 2 in ref. 27). As MCT is eroded over THW, the seismicity can only occur structurally below the level of

the eroded MCT plane and MCT cannot be the active seismogenic fault in DSH. Also, very few epicentres plot north of MCT trace in THW[31–33,42,43], suggesting once again, that MCT is probably not the dominantly active seismogenic structure in the DaSiT wedge. Moreover, MCT has been folded by the younger LHD structure[21] and eroded over THW. As faults get folded by younger footwall faults in fold-thrust belts once they become inactive[44], MCT is unlikely to be an active seismogenic fault in the DaSiT wedge.

If we accept that MCT cannot be the active seismogenic structure that produces the cluster of earthquake epicentres between MCT and MBT, several possibilities arise. First, this cluster is related to MHT[23,28]. However, the spread of hypocentres from near-surface down to MHT (0–20 km; Figure 5)[32], suggests that the seismicity cannot be confined only to one seismogenic fault even if it is postulated that the seismicity occurs on the frontal MBT. Given this, it would be difficult to attribute the entire spread of hypocentres to MBT or MHT. One strong possibility is that the diffused seismicity, that is spread over 0–20 km and deeper between the surface traces of MBT and MCT, is related to an active LHD[20,21,26]. Two facts strongly support this interpretation. First, the epicentres of micro- and moderate earthquakes cluster in DSH (Figure 3) exactly in the region where LHD horses are exposed on the surface. Second, the distribution of hypocentres in the region between MHT and the surface traces of MBT and MCT also coincide with the location of LHD (Figures 4 and 5). Moreover, the cluster of epicentres tapers out both east and west of THW (Figure 3). Therefore, the seismicity pattern more or less mimics the three-dimensional geometry of LHD. Given this, we interpret that the cluster of epicentres and hypocentres in the region between the surface traces of MBT and MCT, as well as above MHT (Figures 3 and 4) is related to a seismogenic LHD in DSH and is likely to be primarily the result of active thrust seismotectonics in the DaSiT Himalayan wedge.

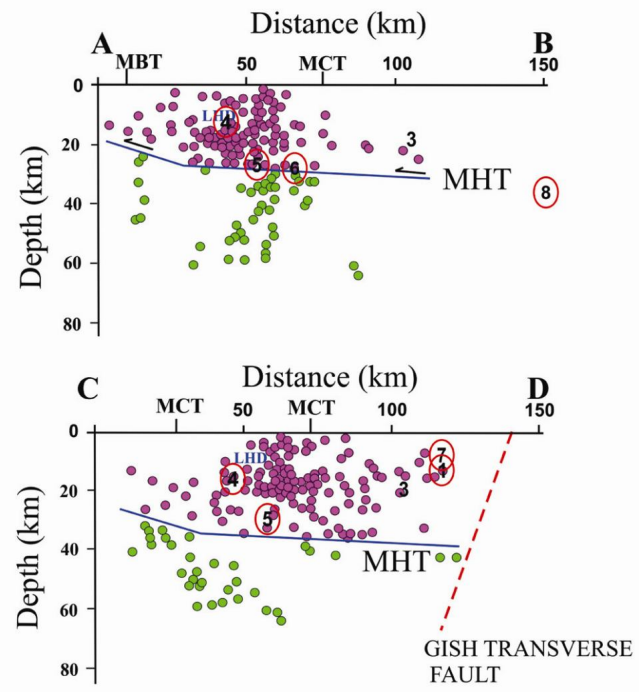

Figure 5. Distribution of hypocentres in DSH[34,35]. It is difficult to visualize that all the purple hypocentres would lie on MHT and given that they are located between MBT and MCT where LHD has been mapped, the LHD appears to be the most appropriate seismogenic structure. The green hypocentres below MHT are most likely to be related to strike–slip tear faults, the Gish Transverse Fault, and cross-structures related to them at both east and west ends of the Dharan salient. The numbers in the section refer to earthquake hypocentres reported in Table 1 and Figure 4. The top and bottom figures are along lines of cross-section AB and CD respectively in Figure 3. Also, the strike–slip earthquakes have been circled in red.

Strike–slip seismotectonics

N–S depth sections across THW[31–33,35,43] reveal that many hypocentres extend to depths of 45 km in the frontal part of DSH (Figures 4 and 5) and depths of even 70 km under LHD[27,35]. This has led to interpretations of an unusually deep MBT that extends below the basal detachment of the Himalaya or MHT into the Moho[33,43]. This interpretation is not consistent with the seismotectonics of rest of the Himalaya, wherein the MBT is recognized as a listric thrust fault that meets MHT at a very low angle or soles with MHT. The earthquake hypocentres also seem to be located north of the MBT surface trace, but for MBT to be the causative fault, it would have to be a very steep fault. However, the deep hypocentre distribution is diffused and distributed over an area between eastern Nepal and the Gish Transverse Fault (GTF)[5] and is too large to support the contention that there is a single seismogenic fault (Figures 4 and 5). Moreover, MBT has been folded in the region by the South Kalijhora Thrust (SKT)[10,45]. As faults get folded by younger footwall faults in fold-thrust belts once they become inactive[44], MBT is also unlikely to be active or seismogenic[10]. The Moho in the region has been interpreted to lie at 40–80 km depth based on the deep earthquakes that are present at that depth[27]. The deep earthquakes at 20–40 km between MHT and the Moho contain several strike–slip earthquakes[27] that suggest the presence of strike–slip faults in the region that extend below MHT or the basal decollement of the DaSiT Himalayan wedge. Having recognized this, known strike–slip earthquakes and fault planes in the region need to be evaluated to postulate a viable kinematic scenario for strike–slip earthquakes that is consistent with modern understanding of along- and across-strike deformation of fold-and-thrust belt kinematics.

Lineaments and strike–slip faulting in DSH

Strike–slip earthquakes have been traditionally attributed to lineaments in DSH (e.g. Tista lineament, Gangtok

lineament, Goalpara lineament; Figures 3 and 4). These lineaments were presumably mapped by remote sensing[46], although it is not clear if field verification of these lineaments was ever carried out or if they even represent actual fault zones. The Tista lineament, as mapped within the mountain front[47], is shown to cross-cut the western part of LHD as well as the thrust sheets. No such fault zone was observed in the field[20,21]. All lineaments are mapped as straight lines (Figure 3) that run through all topographic highs[46,47] and lows and, therefore, have to be vertical faults. The lineaments are also oblique to the transport direction of the thrust-sheets as well as the east-west trend of the major faults. Thus, even if the lineaments really exist, their geometry and kinematic significance is not well-constrained. The only transverse fault in the Darjiling–Sikkim region that has been physically mapped is the NNE–SSW trending GTF[5,48], which is a sinistral strike–slip fault in the zone of transition between the Dharan salient and the Gorubathan recess (Figure 1). The GTF fault zone consists of fault gouge in a zone ~500 m thick dipping steeply to the west and could be the northward extension of the west-dipping Kishanganj fault (for example figure 1 in ref. 42). The 19 November 1980 (*Mb* 6.2) strike–slip event plots in the hanging wall of GTF and one of the nodal planes of the fault-plane solution of the event (NE–SW trending plane) is parallel to the geometry of GTF. The event, however, has been considered to occur on the NW–SE trending nodal plane of the fault plane solution along the Goalpara lineament[42], which is again a lineament not mapped out physically in the field. The Goalpara lineament is an oblique feature to the overall transport direction of the Himalaya, whose kinematics is difficult to explain in the context of the overall kinematics of the Himalaya. In contrast, GTF is a transport-parallel, steep west-dipping, sinistral, strike–slip fault that has been mapped in the field and is related to salient–recess transition between the Dharan salient and the Gorubathan recess. As the geometry and kinematics of GTF are known and consistent with the NE–SW nodal plane of the 19 November 1980 (*Mb* 6.2) strike–slip event, we interpret it to be related to an active and seismogenic GTF occurring in the transition zone between the Dharan salient and the Gorubathan recess. Also, GTF need not be confined to the DaSiT wedge and can extend below MHT, especially if it is related to the Kishanganj basement fault which has been recognized to be a deep-seated fault based on gravity studies[49]. Therefore, we postulate that some of the deep hypocentres (20–40 km) that occur below MHT, particularly near the Dharan salient–Gorubathan recess transition zone are associated with the seismogenic GTF.

Occurrence of strike–slip earthquakes such as the 18 September 2011 (*Mw* 6.9) and 12 January 1965 (*M* 6.1) events in eastern Nepal along with linear alignment of moderate-earthquake epicentres indicates strike–slip activity (Figure 4) along the Kanchenjunga lineament[39–41]. However, the Kanchenjunga lineament is again not a physically mapped fault zone, and the geometry and kinematics of the strike–slip tectonics in eastern Nepal need to be studied further. In accordance with the modern concepts of thrust belt deformation and evolution, a transverse, N–S trending, dextral strike–slip fault is expected at the western edge of the Dharan salient approximately parallel to GTF. The Kanchenjunga lineament could be that fault but that needs to be verified by structural mapping. For now, we can at best postulate that the Dharan salient is bounded by two approximately NNE–SSW trending transverse faults which are seismogenic and are generating moderate strike–slip earthquakes. Further work needs to be carried out to constrain the causative fault in the western part of the Dharan salient.

Global Positioning Studies in the frontal DSH

High-precision GPS measurements were first initiated in the frontal Darjiling Himalaya in 1997 at Delo Hill near Kalimpong town (Table 2). Subsequently, four sites were added west of GTF in 2000 at Labha, Mungpu, Kyongnosla and Namchi. Finally, the first-order network was completed in 2002 with the establishment of the Nim station east of GTF. The Kyongnosla and Nim stations are located on either side of GTF east of the THF window to measure the slip rate on GTF. All the above are campaign-mode stations measured once a year for three continuous days. Campaign sites were marked by 2–3 mm diameter holes drilled on bedrock exposures to allow subsequent re-occupations on bipods. A permanent station was established at Panthang (Gangtok) in 2003 with choke ring antennae mounted on a concrete pillar grouted to bedrock. The sites at Mungpu and Namchi are located away from GTF and in the middle of THW. Thus, the Mungpu–Namchi and the Namchi–Panthang baselines can be used to estimate the convergence accommodated within the seismogenic LHD within THW. The results presented here are based on GPS measurements carried out in DSH during 1997–2006 and continuous 2003–2006 data from the permanent station. The data processing and analysis were carried out using standard procedures[50] and the GAMIT/GLOBK processing software developed by Massachusetts Institute of Technology (MIT), USA[51].

Active tectonics in DSH from Geodetic GPS

GPS measurements allow the estimation of very short-term, active deformation starting from the day a station is setup and measured for the first time. Bangalore (IISc: 13.02N; 77.57E) and Lhasa (LHAS: 29.66N; 91.10E) are two permanent International GPS Service (IGS) stations that are relevant to the study of the deformation in the region because the IISc–Lhasa baseline is a good proxy for deformation in the Darjiling–Sikkim and Western

Table 2. Coordinates and International Terrestrial Reference Frame 2000 velocities of GPS stations during 1997–2006 relevant to the tectonics of the study region

Station	Latitude (°N)	Longitude (°E)	Velocity (E; mm/year)	Velocity (N; mm/year)	Composite velocity (mm/year)
IISC^	13.021	77.570	41.42 ± 0.32	34.52 ± 0.27	53.92 ± 0.30 N50.19 ± 0.31E
LHAS^	29.657	91.104	44.90 ± 0.27	13.22 ± 0.35	46.81 ± 0.28 N73.60 ± 0.42E
GBSK* (2003–2006)	27.365	88.569	37.17 ± 0.36	28.24 ± 0.35	46.68 ± 0.36 N52.78 ± 0.44E
KYON	27.367	88.714	37.73 ± 0.62	26.14 ± 0.46	45.90 ± 0.57 N55.28 ± 0.65E
NAMC	27.157	88.322	36.65 ± 0.48	29.84 ± 0.39	47.26 ± 0.45 N50.85 ± 0.52E
DELO	27.089	88.503	37.02 ± 0.45	29.12 ± 0.38	47.10 ± 0.43 N51.81 ± 0.50E
LAVA	27.070	88.664	36.72 ± 0.45	30.40 ± 0.38	47.67 ± 0.42 N50.38 ± 0.49E
NIMC (2002–2006)	26.998	88.685	36.83 ± 0.85	31.41 ± 0.65	48.41 ± 0.77 N49.54 ± 0.88E
MUNG	26.978	88.400	36.25 ± 0.49	32.03 ± 0.39	48.37 ± 0.45 N48.54 ± 0.52E
Other IGS stations					
KUNM	25.030	102.797	28.06 ± 0.35	–19.25 ± 0.45	
HYDE	17.417	78.551	38.77 ± 0.33	33.62 ± 0.27	
SELE	43.179	77.017	26.34 ± 0.28	01.64 ± 0.24	
KIT3	39.135	66.885	26.55 ± 0.25	03.86 ± 0.19	
BAHR	26.209	50.608	30.90 ± 0.23	28.59 ± 0.23	
POL2	42.680	74.694	26.33 ± 0.28	03.36 ± 0.23	

*Permanent; ^IGS station.

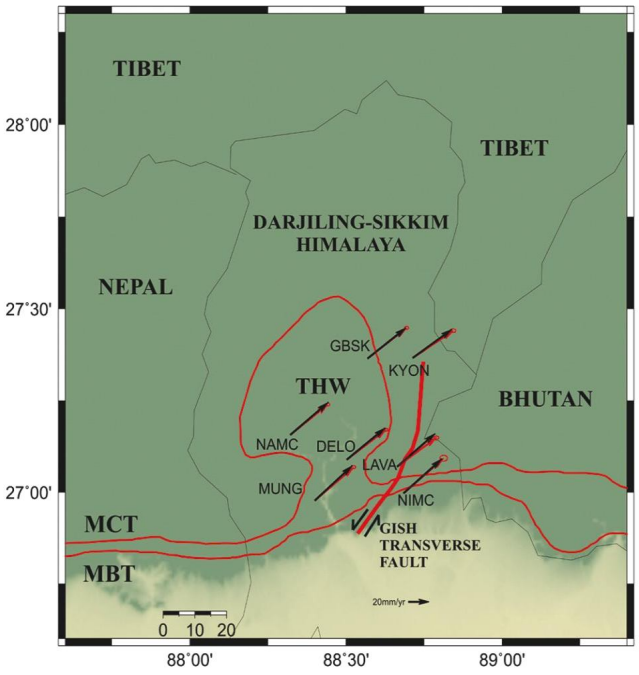

Figure 6. Location of the permanent station at Panthang (GBSK) and campaign mode GPS stations in DSH at Labha (LAVA), Nim (NIMC), Kyongnosla (KYON), Delo Hill (DELO), Namchi (NAMC) and Mungpu (MUNG) along with their measured velocity vectors in ITRF 2000 reference frame. THW and GTF are also shown. Red arrows represent the velocities reported earlier[48], while black arrows represent the velocities between 1997 and 2006 used in the present analysis.

Bhutan Himalayas. The IISc velocity (53.92 ± 0.30N; 50.19 ± 0.31E) is representative of the Indian plate, whereas the Lhasa velocity (46.81 ± 0.28N; 73.60 ± 0.42E) is indicative of predominantly easterly motion characteristic of the Tibetan plate. The computed IISc–LHAS baseline shortening for the period 1997–2006 is 12.97 ± 0.11 mm/year (Table 3), which is less compared to its west (~ 20 mm/year)[28] in central Nepal and east (~ 16 mm/year)[50] in central Bhutan.

The velocities measured in the frontal part of DSH at Mungpu and Nim west and east of GTF (Table 2; Figure 6) indicate that the Indian plate slows down to ~ 48 mm/year from ~ 54 mm/year at Bangalore. This indicates that ~ 6 mm/year of shortening is accommodated in eastern peninsular India. The campaign station at Mungpu and the permanent station at Panthang are located approximately at the south and north ends of THW where maximum seismicity is observed in DSH. The velocity at Panthang is only 1.69 ± 0.58 mm/year lower than at Mungpu (Table 2; Figure 6), which indicates that some strain is accumulating in THW; the Mungpu–Panthang baseline shows shortening of ~ 3 mm/year (Table 3). Both these stations are located in the west block of GTF. They are also located away from the fault zone. Therefore, they are likely to represent shortening that is being accommodated along active east-west trending faults in LHD in THW. Namchi is a campaign-mode station located at the

Table 3. GPS convergence (shortening) rates during 2000–2006 in the Darjiling–Sikkim Himalaya

Baseline	2006 length (m)	Convergence (mm/year)
IISc-LHAS	2299529.1468 ± 0.0007	–12.97 ± 0.11
IISc-KYON	1959695.1528 ± 0.0017	–07.82 ± 0.53
IISc-GBSK (2003–2006)	1950581.7891 ± 0.0008	–06.13 ± 0.23
IISc-LAVA	1930950.8238 ± 0.0011	–05.11 ± 0.33
IISc-DELO	1922731.3908 ± 0.0020	–04.98 ± 0.34
IISc-NAMC	1917600.2625 ± 0.0013	–04.83 ± 0.36
IISc-MUNG	1906750.2355 ± 0.0011	–04.30 ± 0.36
IISc-NIMC (2002–2006)	1925927.6783 ± 0.0016	–04.51 ± 0.87
LHAS-KYON	0345298.7524 ± 0.0013	–05.01 ± 0.44
LHAS-GBSK (2003–2006)	0355188.2906 ± 0.0005	–05.70 ± 0.20
LHAS-LAVA	0373517.3734 ± 0.0008	–08.26 ± 0.28
LHAS-DELO	0382192.2169 ± 0.0017	–06.78 ± 0.30
LHAS-NAMC	0388813.7616 ± 0.0010	–06.35 ± 0.32
LHAS-MUNG	0398197.6755 ± 0.0009	–08.65 ± 0.31
LHAS-NIMC (2002–2006)	0378429.9479 ± 0.0011	–09.44 ± 0.67
KYON-GBSK (2003–2006)	0014407.0339 ± 0.0016	00.26 ± 0.62
KYON-LAVA	0033353.8381 ± 0.0013	–04.07 ± 0.37
KYON-DELO	0037293.4824 ± 0.0020	–02.31 ± 0.50
KYON-NAMC	0045374.4576 ± 0.0017	–01.20 ± 0.62
KYON-MUNG	0053305.2446 ± 0.0015	–03.87 ± 0.51
KYON-NIMC (2002–2006)	0041125.8547 ± 0.0015	–05.13 ± 0.69
GBSK-LAVA (2003–2006)	0034051.2708 ± 0.0007	–02.23 ± 0.26
GBSK-DELO (2003–2006)	0031309.1895 ± 0.0013	–00.85 ± 0.26
GBSK-NAMC (2003–2006)	0033695.4375 ± 0.0014	–00.75 ± 0.37
GBSK-MUNG (2003–2006)	0046157.1749 ± 0.0008	–03.09 ± 0.29
GBSK-NIMC (2003–2006)	0042334.2822 ± 0.0011	–03.10 ± 0.60
LAVA-DELO	0016095.2786 ± 0.0022	–00.60 ± 0.51
LAVA-NAMC	0035263.9996 ± 0.0013	–00.25 ± 0.52
LAVA-MUNG	0028110.7975 ± 0.0012	–00.16 ± 0.51
LAVA-NIMC (2002–2006)	0008338.0923 ± 0.0014	–00.75 ± 0.76
DELO-NAMC	0019475.7815 ± 0.0017	00.58 ± 0.51
DELO-MUNG	0016061.3900 ± 0.0019	–01.36 ± 0.43
DELO-NIMC (2002–2006)	0020707.2851 ± 0.0022	–01.04 ± 0.83
NAMC-MUNG	0021369.4391 ± 0.0011	–02.04 ± 0.31
NAMC-NIMC (2002–2006)	0040102.5839 ± 0.0015	–00.56 ± 0.83
MUNG-NIMC (2002–2006)	0028330.5143 ± 0.0015	00.46 ± 0.88

centre of THW as well as within the Lower Himalayan Rangit Duplex in DSH and away from the trace of GTF. The Mungpu–Namchi baseline has shortened by 2.04 ± 0.31 mm/year during 2000–2006 (Table 3), indicating that most of the shortening in THW is accommodated in its southern part. Kyongnosla, however, is located very close to GTF fault zone in the hanging wall of the fault and the Mungpu–Kyongnosla baseline shows a shortening of ~4 mm/year. Therefore, a maximum of ~4 mm/year shortening is accommodated in THW or LHD west of the surface trace of GTF in the Dharan salient; this is expressed as micro- to moderate earthquakes within THW.

Quantification of present-day slip rate on GTF

Five campaign-mode stations were set up to determine the slip on GTF (Figure 6). The campaign-mode stations at Labha (LAVA: 27.07N, 88.66E) and Kyongnosla (KYON: 27.36N; 88.71E) were set-up very close to the surface trace of GTF (Figure 6). Delo Hill (DELO: 27.09N; 88.50E), Mungpu (MUNG: 26.98N; 88.40E), Namchi (NAMC: 27.16N; 88.32E) and Panthang (GBSK: 27.365N; 88.569E) were set-up away from the GTF surface trace. All the above stations were set-up west of the surface trace of GTF in the Dharan salient. Nim (NIMC: 26.99N; 88.68E) was the only station set-up east of GTF surface trace in the Gorubathan recess because of logistical problems related to close proximity of international borders east of GTF. We look at velocities of all these stations relative to the Nim station to work out the slip-rate on GTF (Table 4; Figure 7) during 2000–2006. Mungpu and Lava, which are located west of GTF surface trace at the same latitude as Nim, do not exhibit any significant relative motion with Nim (Table 4; Figure 7). This indicates that GTF, along with the rest of the frontal DSH, is locked (Figure 7) south of 27°N lat. North of 27°N, Delo Hill and Namchi exhibit a southward relative velocity of 1.5–2.3 mm/year relative to Nim. Panthang, however, exhibits a higher southward relative velocity of ~3 mm/year (Table 4). The northernmost station at Kyongnosla records ~5 mm/year (fault-parallel component 3.40 ± 0.43 mm/year) southward velocity relative to Nim (Table 4; Figure 7). This indicates that there is

Table 4. Velocities of GPS stations relative to NIMC and GBSK

Station	Velocity (E; mm/year) NIMC fixed	Velocity (N; mm/year) NIMC fixed	Velocity (E; mm/year) GBSK fixed	Velocity (N; mm/year) GBSK fixed
GBSK (2003–2006)*	0.34 ± 0.82	–3.17 ± 0.58	0	0
KYON	0.89 ± 0.96	–5.26 ± 0.65	0.55 ± 0.59	–2.09 ± 0.35
NAMC	–0.18 ± 0.88	–1.57 ± 0.60	–0.52 ± 0.45	1.60 ± 0.25
DELO	0.19 ± 0.88	–2.28 ± 0.60	–0.15 ± 0.44	0.89 ± 0.24
LAVA	–0.12 ± 0.84	–1.01 ± 0.60	–0.46 ± 0.41	2.16 ± 0.24
NIMC (2002–2006)	0	0	–0.34 ± 0.82	3.17 ± 0.58
MUNG	–0.58 ± 0.88	0.62 ± 0.60	–0.92 ± 0.46	3.79 ± 0.25

*Permanent station.

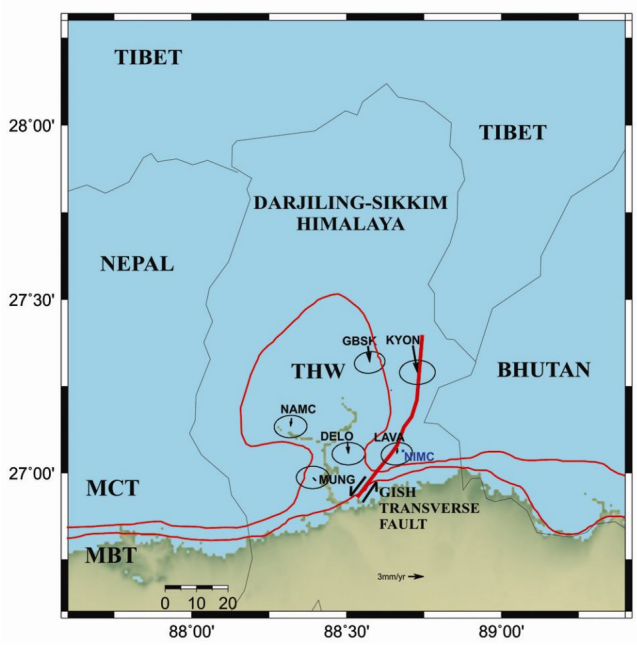

Figure 7. Southward motion of the west block of GTF relative to the east block is evident from velocity vectors plotted with a fixed Nim campaign station (NIMC). The locked part of GTF is evident from very small relative motion between Nim and Mungpu (MUNG). Slip of around 3–4 mm/year is evident along GTF.

about 3–4 mm/year slip on GTF between 2000 and 2006 north of 27.07°N and it is locked south of 27°N. Moreover, as the west block of the fault moves to the south relative to the east block, the slip on GTF is sinistral or left-lateral. As mentioned earlier, sinistral strike–slip earthquakes have been recorded near Kyongnosla (Figures 4 and 5; Table 1) which corroborates the GPS results and additionally indicates that the slip on GTF is seismogenic and produces moderate strike–slip earthquakes.

Dislocation modelling of observed GPS velocities in DSH

India-fixed velocities for the Sikkim sites are determined using pole of rotation defined by lat. 51.7 ± 0.5°, long. –15.1 ± 1.5° and angular velocity 0.469 ± 0.01°/Myr (ref. 50). Dislocation modelling was carried out to model the causative fault(s) that could have produced these observed India-fixed displacements (Table 5; Figure 8) using a forward modelling approach. The causative fault was modelled as a finite rectangular dislocation using boundary element method[52] and 3D Green's functions in an elastic half-space with uniform isotropic elastic properties[53,54] in Coulomb 3.3 (refs 55, 56).

We first seek a single dislocation as the possible causative fault and try to simulate measured India-fixed velocities representing the back-slip in DSH (Table 5). A single dislocation is chosen to simulate slip along MHT with a maximum strike-parallel length of ~75 km distance between the boundaries of the Dharan salient defined by the surface trace of GTF to the east near NIMC and the epicentre of the 2011 Sikkim earthquake to the west (Figure 8 *a*). The strike-parallel length, dip and the depth of the dislocation were varied between 50 and 72 km, 7°N and 9°N and 12 and 18 km respectively, to stimulate the slip along MHT in the frontal DSH (Table 5; Figure 8)[13]. The locking line can be placed at 27°N, ~ 10 km north of the mountain front and just south of MUNG and NIMC which show statistically insignificant India-fixed velocity. More weightage was given to the velocity measured at the permanent station GBSK. A top-to-the-south reverse slip of 4–5 mm/year along the dislocation at 18 km depth was used to simulate the GBSK north velocity. The best results were obtained with a 7°N dip and top-to-the-south slip of 4 mm/year (case I; Table 5). However, velocities at all other stations (with the exception of KYON) are overestimated. Moreover, all stations also exhibit 2–4 mm/year of east velocity that is not simulated by the above model. We attempted to simulate the measured east velocities using an oblique-slip model on the dislocation above by introduction of an additional 3 mm/year strike–slip motion on the dislocation plane from east to west (case II; Table 5). The oblique-slip model simulates the measured east and north velocities better (Figure 8 *a*). We tested this further by varying the dip, the slip as well as the strike-parallel length of the dislocation. The modelled velocities closest to the measured velocity field were obtained in case III (Table 5; Figure 8 *b*). However, measured velocities at KYON continued to be underestimated in all models. The north velocities of other stations were overestimated by all the variations used in the

Table 5. Single/multiple-fault dislocation model with five different combinations of model parameters

	Observed velocity (mm/year)		I		II (Figure 8 *a*)		III (Figure 8 *b*)		IV		V (Figure 9)	
Code	E	N	E	N	E	N	E	N	E	N	E	N
KYON	–2.21 ± 0.62	–5.26 ± 0.46	–0.17	–2.73	–1.72	–2.53	–1.83	–2.47	–1.70	–1.78	–2.07	–4.01
NIMC	–3.18 ± 0.85	0.01 ± 0.65	0.12	0.11	0.14	–0.02	–0.07	–0.12	0.12	0.07	–0.75	–0.19
LAVA	–3.27 ± 0.45	–1.01 ± 0.38	–0.28	–3.52	–2.73	–3.17	–3.27	–3.73	–1.29	–1.17	–2.28	–2.09
GBSK	–2.74 ± 0.36	–3.18 ± 0.35	–0.31	–3.26	–2.53	–3.03	–2.81	–3.28	–2.96	–3.08	–2.92	–3.42
DELO	–2.93 ± 0.45	–2.31 ± 0.38	–0.40	–3.63	–3.14	–3.29	–3.97	–3.89	–2.91	–2.10	–3.28	–2.31
MUNG	–3.70 ± 0.49	0.59 ± 0.39	0.03	0.23	0.17	0.22	0.27	0.38	0.23	0.35	0.07	0.16
NAMC	–3.24 ± 0.48	–1.61 ± 0.39	–0.44	–3.61	–3.17	–3.28	–3.96	–3.82	–2.91	–2.04	–3.22	–2.09

Sl. no.	Fault type	Length (km)	Width (km)	Depth (km)	Dip (°)	Strike–slip (mm)	Reverse slip (mm)
Model parameters							
I	Reverse slip	72	147.70	18	7	0	4
II	Oblique slip	72	147.70	18	7	3	4
III	Oblique slip	50	76.41	12	9	4	5
IV	Oblique slip	68	63.92	10	9	3	3
	Oblique slip	72	46.36	12	15	1	2
V	Oblique slip	70	63.92	10	9	3	3
	Strike–slip	35	30.89	28	65	4	0
	Oblique slip	72	41.04	12	17	1	2

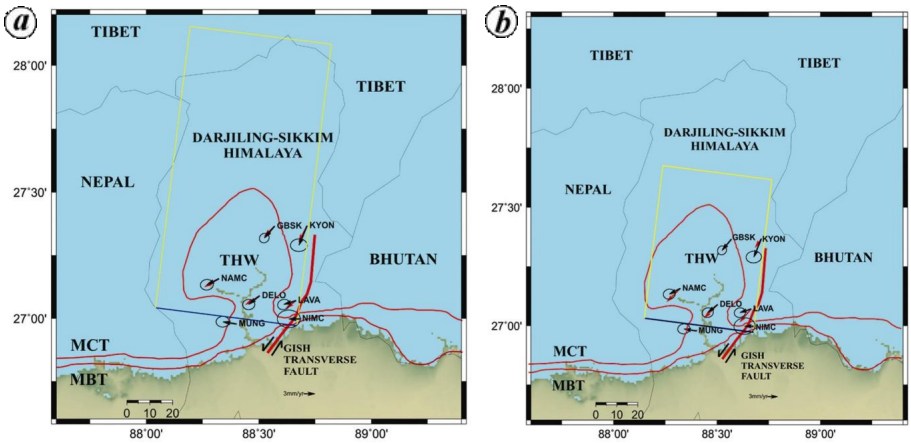

Figure 8. Velocities obtained from dislocation modelling using a single dislocation simulating slip on MHT as a thrust fault with oblique slip with parameters (***a***) Case II and (***b***) Case III (Table 5). Measured velocities at KYON are underestimated and north velocities of other stations overestimated by this model. This suggests that a single dislocation, corresponding to a frontal MHT, with reverse or oblique slip, is not able to simulate measured values accurately and more complex models need to be explored to simulate the measured velocities in DSH.

model. This suggests that a single dislocation, corresponding to a frontal MHT, with reverse or oblique slip, is not able to simulate measured values accurately and more complex models need to be explored to simulate the measured velocities in DSH.

A two-dislocation thrust-fault model was next attempted, wherein an additional dislocation was added to the frontal dislocation near LHD south of NAMC. The dip of the second dislocation was taken to be higher (15°) to simulate the greater dip of MHT in the middle part of the DSH wedge. The two-dislocation model simulates GBSK and DELO India-fixed north velocities accurately when only reverse-slip is used and India-fixed east and north velocities when oblique slip is used. Underestimation of KYON and overestimation of LAVA and NAMC India-fixed velocities continue to occur. However, in the best two-fault dislocation model (case IV; Table 5) overestimated values are closer to the measured values compared to the one-fault dislocation model. This seems to indicate that active deformation in DSH may not be confined to a single fault or MHT[17,28] and LHD may also be actively deforming. In addition, the unusually high India-fixed velocity of KYON cannot be simulated by one or two thrust dislocation models. As KYON lies in the hanging wall and is close to the surface trace of GTF, slip along GTF probably also contributed to the India-fixed velocity of KYON. We therefore explore the effect of an additional strike–slip fault with parameters as close to the rupture parameters of the 19 November 1980 strike–slip earthquake as possible using a three-dislocation model

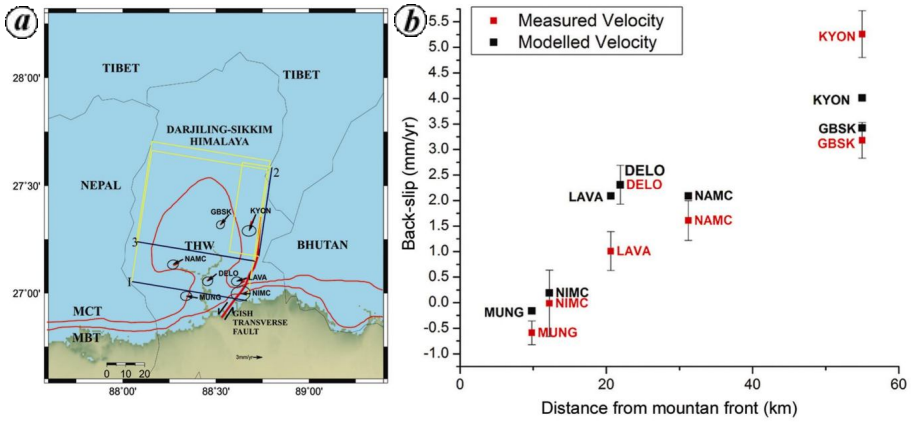

Figure 9. ***a***, Dislocation model using three dislocations simulating two thrust faults with oblique slip and one strike–slip fault. ***b***, The resultant modelled velocities were closest to the overall measured India-fixed, back-slip velocity field (Table 5) in the frontal DSH indicating that this is the most realistic out of the three models attempted here. However, more detailed measured velocity field needs to be simulated by dislocation modelling to understand how the back-slip is distributed in the Darjiling–Sikkim–Tibet Himalayan wedge.

with two thrust faults and one strike–slip fault (Figure 9 *a*). The resultant modelled velocities were the closest we could get to the overall measured India-fixed, back-slip velocity field (case V; Table 5) in the frontal DSH (Figure 9 *b*).

The forward modelling using boundary element method suggests that the India-fixed velocities measured in the frontal DSH are unlikely to be simulated by a single dislocation with thrust-slip (that represents MHT)[17,28]. We need a denser network of high-precision GPS stations to explore this further. The dislocation model that seems to simulate measured India-fixed velocities or back-slip in the frontal DSH most closely is oblique-slip along two thrust dislocations and sinistral strike–slip along a strike–slip dislocation (case V; Table 5; Figure 9). These results seem to be consistent with geological insights available from the area which suggests active out-of-sequence deformation in the frontal Himalaya near the MBT surface trace[29] and LHD[5], in addition to slip along the basal decollement (MHT) and strike–slip motion along GTF[5]. Nevertheless, a denser network with more high-precision GPS stations, particularly from the northern and western part of DSH is required to address the question of how the active slip along the basal decollement is being distributed within DSH.

Discussion

The DSH extends from Nepal in the west to Bhutan in the east. Geologically, the western DSH is located in the Dharan salient and the eastern DSH in the Gorubathan recess[5]. As evident from the seismicity, geology and dislocation modelling, the Dharan salient is bounded by two strike–slip faults; the eastern fault, i.e. GTF, is sinistral, dips steeply to the west, and has been mapped from the Himalayan foreland to the Yadong-Gulu rift[5,48]. The geometry and kinematics of the western fault have not been worked out yet, but the seismicity patterns in the western Dharan salient point to a roughly NE–SW trending, steep-dipping, dextral main fault with possible active cross-faults[57]. Active seismicity in DSH, as evident from available seismic data, appears to be largely confined to the frontal physiographic THW where LHD is located. However, high-precision GPS measurements using long time-series (between 1997 and 2006) and short baseline lengths (Table 5) reveal that only about 3–4 mm/year of convergence is being accommodated in the seismogenic THW and LHD. The frontal DSH south of THW is locked both in the Dharan salient and the Gorubathan recess and does not accommodate any statistically significant strain.

Active deformation in DSH is partitioned into two distinct mechanisms. First, seismogenic sinistral strike–slip on GTF at the rate of about 3–4 mm/year. Earthquakes related to this can have deep hypocentres and extend to depths below the Himalayan basal decollement (MHT) as GTF is postulated to be the northern extension of the deep-seated Kishanganj fault[49]. These hypocentres are also likely to be located west of the surface trace of GTF as it is a near-vertical, west-dipping fault. Second, active seismogenic thrust deformation on E–W striking faults predominantly in THW, but extending also to the east of the surface trace of GTF in the Gorubathan recess, is also observed in DSH. The source of these earthquakes is unresolved except that MBT and MCT are unlikely to be seismogenic in THW or the Gorubathan recess. The diffused nature of the seismicity also suggests that it is likely to be related to more than one seismogenic fault and may point to out-of-sequence and/or reactivated faults in LHD or MHT. This is also supported by the uneven distribution of the lithospheric heterogeneities having variable *b*-values (0.74–1.18) and mixed types of faulting obtained through composite fault-plane solution for different blocks in the study area of DSH[26]. The thrust-related seismicity in THW occurs in response to the accommodation of its ~3 mm/year shortening.

The nature of active tectonics in DSH indicates many deviations from the recognized models of Himalayan deformation. For example, only about 12 mm/year of convergence is accommodated across DSH and western Bhutan Himalaya. About 3–4 mm/year of this convergence is accommodated by strike–slip along GTF and 3 mm/year is accommodated along east-west faults. This also means that about 5 mm/year of aseismic (?) slip is being taken up north of THW. Presence of active transport-parallel transverse faults such as GTF in the Himalaya also suggests that active deformation in the Himalayan arc is not continuous and different parts of the arc may be accommodating different amounts of convergence partitioned into several mechanisms. Seismicity patterns along the length of the arc also seem to be discontinuous and different parts of the belt seem to be active at different places along the length of the arc[23], suggesting that the Himalayan deformation may be segmented into blocks along the length of the mountain belt that tend to move and deform as separate units[58,59]. Transverse zones have also been observed elsewhere in the Himalayas[60,61] and major rivers such as Ganga and Yamuna seem to follow these zones before they exit into the Himalayan foreland. It follows that the deformation kinematics of each of these blocks needs to be worked out separately and put together to construct the signatures of the overall Himalayan deformation. Given this, cobbling together of geological sections, Quaternary deformation signatures and GPS convergence rates from different parts of the Himalaya across such transverse zones should be avoided. For example, the results of the INDEPTH Project[12] have been extrapolated to different parts of the Himalaya to prepare representative sections across the Himalaya even though the INDEPTH work is representative of the Himalayan hinterland only north of DSH. Similarly, present-day convergence rate of ~20 mm/year measured in the Nepal Himalaya has been extrapolated to other parts of the Himalayan arc[28]. The rates measured in the Nepal Himalaya are representative of only the central Nepal Himalaya and not necessarily everywhere in the Himalayan arc. Given all this, the role of transverse zones in Himalayan deformation may be significant and must be therefore studied and better understood. These observations suggest that a fresh look at our ideas on the Himalayan deformation is required as it appears to be more complex than visualized by the current models.

1. Bendick, R. and Bilham, R., How perfect is the Himalayan arc? *Geology*, 2001, **29**(9), 791–794.
2. Macedo, J. and Marshak, S., The geometry of fold-thrust belt salients. *Geol. Soc. Am. Bull.*, 1999, **111**, 1808–1822.
3. Marshak, S., Arcs, oroclines, salients, and syntaxes – the origin of map-view curvature in fold-thrust belts. *Am. Assoc. Pet. Geol. Mem.*, 2004, **82**, 131–156.
4. Powers, P. M., Lillie, R. J. and Yeats, R. S., Structure and shortening of the Kangra and Dehra Dun reentrants, Sub-Himalaya, India. *Geol. Soc. Am. Bull.*, 1998, **110**, 1010–1027.
5. Mukul, M., First-order kinematics of wedge-scale active Himalayan deformation: insights from Darjiling–Sikkim–Tibet (DaSiT) wedge. *J. Asian Earth Sci.*, 2010, **39**, 645–657.
6. Dasgupta, S., Mazumdar, K., Moirangcha, L. H., Gupta, T. D. and Mukhopadhyay, B., Seismic landscape from Sarpang re-entrant, Bhutan Himalaya foredeep, Assam, India: constraints from geomorphology and geology. *Tectonophysics*, 2013, **592**, 130–140.
7. Dubey, A. K., Mishra, R. and Bhakuni, S. S., Erratic shortening from balanced cross sections of the western Himalayan foreland basin causes and implications for basin evolution. *J. Asian Earth Sci.*, 2001, **19**, 765–777.
8. Yin, A., Cenozoic tectonic evolution of the Himalayan orogen as constrained by along strike variation of structural geometry, exhumation history, and foreland sedimentation. *Earth-Sci. Rev.*, 2006, **76**, 1–131.
9. Sahoo, P. K., Kumar, S. and Singh, R. P., Neotectonic study of Ganga and Yamuna tear faults, NW Himalaya, using remote sensing and GIS. *Int. J. Remote Sensing*, 2000, **21**(3), 499–518.
10. Mukul, M., The geometry and kinematics of the Main Boundary Thrust and related neotectonics in the Darjiling Himalayan fold-and-thrust belt, West Bengal. *J. Struct. Geol.*, 2000, **22**(9), 1261–1283.
11. Barnes, J. B., Densmore, A. L., Mukul, M., Sinha, R., Jain, V. and Tandon, S. K., Interplay between faulting and base level in the development of Himalayan frontal fold topography. *J. Geophys. Res., F: Earth Surf.*, 2011, **116**, F03012; doi: 10.1029/2010JF001841.
12. Schelling, D. and Arita, K., Thrust tectonics, crustal shortening, and the structure of the far-eastern Nepal Himalaya. *Tectonics*, 1991, **10**, 851–862.
13. Nelson, K. D. *et al.*, Partially molten middle crust beneath southern Tibet: synthesis of project INDEPTH results. *Science*, 1996, **274**, 1684–1688.
14. Srivastava, P. and Mitra, G., Thrust geometries and deep structure of the outer and lesser Himalaya, Kumaon and Garhwal (India): implications for evolution of the Himalayan fold-and-thrust belt. *Tectonics*, 1994, **13**, 89–109.
15. DeCelles, P. G., Gehrels, G. E., Quade, J. and Ojha, T. P., Eocene – early Miocene foreland basin development and the history of Himalayan thrusting, western and central Nepal. *Tectonics*, 1998, **17**, 741–765.
16. Gansser, A., *Geology of the Bhutan Himalaya*, Birkhauser Verlag, Basel, 1983, p. 181.
17. Lavé, J. and Avouac, J. P., Fluvial incision and tectonic uplift across the Himalayas of central Nepal. *J. Geophys. Res. B: Solid Earth*, 2001, **106**(B11), 26561–26591.
18. Boyer, S. E., Sedimentary basin taper as a factor controlling the geometry and advance of thrust belts. *Am. J. Sci.*, 1995, **295**, 1220–1254.
19. Hauck, M. L., Nelson, K. D., Brown, L. D., Zhao, W. and Ross, A. R., Crustal structure of the Himalayan orogen at ~90° east longitude from Project INDEPTH deep reflection profiles. *Tectonics*, 1998, **17**, 481–500.
20. Bhattacharyya, K., and Mitra, G., A new kinematic evolutionary model for the growth of a duplex – an example from the Rangit duplex, Sikkim Himalaya, India. *Gondwana Res.*, 2009, **16**, 697–715.
21. Mitra, G., Bhattacharyya, K. and Mukul, M., The Lesser Himalayan Duplex in Sikkim: Implications for variations in Himalayan shortening. *J. Geol. Soc. India*, 2010, **75**, 276–288.
22. Ni, J. and Barazangi, M., Seismotectonics of the Himalayan collision zone: geometry of the underthrusting Indian plate beneath the Himalaya. *J. Geophys. Res.*, 1984, **89**(B2), 1147–1163.
23. Pandey, M. R., Tandulkar, R. P., Avouac, J. P., Vergne, J. and Heritier, Th., Seismotectonics of the Nepal Himalaya from a local seismic network. *J. Asian Earth Sci.*, 1999, **17**, 703–712.
24. Monsalve, G., Sheehan, A., Schulte-Pelkum, V., Rajaure, S., Pandey, M. R. and Wu, F., Seismicity and one-dimensional velocity structure of the Himalayan collision zone: earthquakes in the crust and upper mantle. *J. Geophys. Res.*, 2006, **111**, B10301; doi: 10.1029/2005JB004062.

25. Mahesh, P., Rai, S. S., Sivaram, K., Paul, P., Gupta, S., Sarma, R. and Gaur, V. K., One-dimensional reference velocity model and precise locations of earthquake hypocenters in the Kumaon–Garhwal Himalaya. *Bull. Seismol. Soc. Am.*, 2013, **103**, 328–339.
26. Mishra, O. P., Chakrabortty, G. K., Singh, O. P., Ghosh, D. C., Mukherjee, K. K. and Das, P. C., A report on seismogenesis in the Sikkim–Darjiling Himalayas and assimilation of dynamic snap shots of the region: future vulnerability. GSI Report (FSP: SEI/CHQ/CGD/2007/070), 2010, p. 57.
27. de la Torre, T. L., Monsalve, G., Sheehan, A. F., Sapkota, S. and Wu, F., Earthquake processes of the Himalayan collision zone in eastern Nepal and the southern Tibetan Plateau. *Geophys. J. Int.*, 2007, **171**, 718–738.
28. Bilham, R., Gaur, V. K. and Molnar, P., Himalayan seismic hazard. *Science*, 2001, **293**, 1442–1444.
29. Mukul, M., Jaiswal, M. and Singhvi, A. K., Timing of recent out-of-sequence active deformation in the frontal Himalayan wedge: insights from the Darjiling sub-Himalaya, India. *Geology*, 2007, **35**(11), 999–1003.
30. De, R., A microearthquake survey in the Himalayan Foredeep Region, North Bengal area. *J. Himalayan Geol.*, 1996, **17**, 71–79.
31. De, R., A microearthquake survey at the main boundary thrust in Sikkim Himalaya. *J. Geophys.*, 2000, **XXI**, 77–84.
32. De, R. and Kayal, J. R., Seismic activity at the MCT in the Sikkim Himalaya. *Tectonophysics*, 2004, **386**, 243–248.
33. Nath, S. K., Vyas, M., Pal, I. and Sengupta, P., A seismic hazard scenario in the Sikkim Himalaya from seismotectonics, spectral amplification, source parameterization and spectral attenuation laws using strong motion seismometry. *J. Geophys. Res. – Solid Earth*, 2005, **110**, B01301; doi: 10.1029/2004JB003199.
34. Hazarika, P. and Kumar, M. R., Seismicity and source parameters of moderate earthquakes in Sikkim Himalaya. *Nat. Hazards*, 2012, **62**, 937–952.
35. Raju, P. S., Rao, N. P., Singh, A. and Kumar, M. R., The 14 February 2006 Sikkim earthquake of magnitude 5.3. *Curr. Sci.*, 2007, **93**, 848–850.
36. Hazarika, P., Kumar, M. R., Srijayanthi, G., Raju, P. S., Rao, N. P. and Srinagesh, D., Transverse tectonics in the Sikkim Himalaya: evidence from seismicity and focal-mechanism data. *Bull. Seismol. Soc. Am.*, 2010, **100**, 1816–1822.
37. Baranowski, J., Armbruster, J., Seeber, L. and Molnar, P., Focal depths and fault plane solutions of earthquakes and active tectonics of the Himalaya. *J. Geophys. Res.*, 1984, **89**, 6918–6928.
38. Ekstrom, G. A., Broad band method of earthquake analysis. Ph D thesis, Harvard University, Cambridge, Mass, USA, 1987.
39. Rajendran, K., Rajendran, C. P., Thulasiraman, N., Andrews, R. and Sherpa, N., The 18 September 2011, North Sikkim earthquake. *Curr. Sci.*, 2011, **101**, 1475–1479.
40. Kumar, M. R., Hazarika, P., Prasad, G. S., Singh, A. and Saha, S., Tectonic implications of the September 2011 Sikkim earthquake. *Curr. Sci.*, 2012, **102**(5), 788–792.
41. Kayal, J. R., Baruah, S., Baruah, S., Gautam, J. L., Arefiev, S. S. and Tatevossian, R., The September 2011 Sikkim deeper centroid *Mw* 6.9 earthquake: role of transverse faults in eastern Himalaya. *DST-DCS Newslett.*, 2011, **21**(2), 13–16.
42. De, R. and Kayal, J. R., Seismotectonic model of the Sikkim Himalaya: constraint from microearthquake surveys. *Bull. Seismol. Soc. Am.*, 2003, **93**, 1395–1400.
43. Kayal, J. R., Microearthquake activity in some parts of the Himalaya and the tectonic model. *Tectonophysics*, 2001, **339**, 331–351.
44. Boyer, S. E. and Elliott, D., Thrust systems. *Am. Assoc. Pet. Geol.*, 1982, **66**, 1196–1230.
45. Basak, K. and Mukul, M., Deformation mechanisms in the South Kalijhora Thrust and thrust sheet in the Darjiling Himalayan fold-and-thrust belt, West Bengal, India. *Indian J. Geol.*, 2002, **72**, 143–152.
46. Nandy, D. R. *et al.* (eds), *Bihar-Nepal Earthquake, 20 August 1988*, Geology Survey of India, Spec. Publ., 1993, vol. 31, p. 104.
47. Dasgupta, S. *et al.*, *Seismotectonic Atlas of India and its Environs*. (eds Narula, P. L., Acharyya, S. K. and Banerjee, J.), Geological Survey of India, 2000, p. 87.
48. Mukul, M., Jade, S. and Matin, A., Active deformation in the Darjiling–Sikkim Himalaya based on 2000–2004 geodetic global positioning system measurements. In *Numerical Methods and Models in Earth Science* (eds Ghosh, P. and Gangopadhyay, S.), Indian Statistical Institute Platinum Jubilee, New India Publishing Agency, New Delhi, 2009, pp. 1–28.
49. Choudhury, S. K. and Dutta, A. N., Crustal thickness in North India and Himalayan region and its geological significance. *Geophys. Res. Bull.*, 1975, **13**, 29–37.
50. Jade, S. *et al.*, Estimates of interseismic deformation in Northeast India from GPS measurements. *Earth Planet. Sci. Lett.*, 2007, **263**, 221–234.
51. King, R. W. and Bock, Y., Documentation of the GAMIT GPS analysis software. Massachusetts Institute of Technology, Cambridge, Mass., USA, 2000.
52. Crouch S. L. and Starfield A. M., *Boundary Element Method in Solid Mechanics*, George Allen & Unwin, London, 1983, p. 322.
53. Okada, Y., Internal deformation due to shear and tensile faults in a half-space. *Bull. Seismol. Soc. Am.*, 1992, **82**(2), 1018–1040.
54. Christensen, N. I., Poisson ratio and crustal seismology. *J. Geophys. Res.*, 1996, **101**(B2), 3139–3156.
55. Lin, J. and Stein, R. S., Stress triggering in thrust and subduction earthquakes, and stress interaction between the southern San Andreas and nearby thrust and strike–slip faults. *J. Geophys. Res.*, 2004, **109**, B02303; doi: 10.1029/2003JB002607.
56. Toda, S., Stein, R. S., Richards-Dinger, K. and Bozkurt, S., Forecasting the evolution of seismicity in southern California: animations built on earthquake stress transfer. *J. Geophys. Res.*, 2005, **110**, B05S16; doi: 10.1029/2004JB003415.
57. Pradhan, R., Prajapati, S. K., Chopra, S., Kumar, A., Bansal, B. K. and Reddy, C. D., Causative source of *Mw* 6.9 Sikkim–Nepal border earthquake of September 2011: GPS baseline observations and strain analysis. *J. Asian Earth Sci.*, 2013, **70–71**, 179–192.
58. Gaur, V. K., Evaluation of seismic hazard in India towards minimizing earthquake risk. *Curr. Sci.*, 1994, **67**, 324–335.
59. Guptasarma, D., Is the seismic risk similar everywhere along the Himalayan collision Belt? *Himalayan Geol.*, 1996, **17**, 1–9.
60. Valdiya, K. S., Himalayan transverse faults and folds and their parallelism with subsurface structures of North Indian Plains. *Tectonophysics*, 1976, **32**, 353–386.
61. Dubey, A. K., Bhakuni, S. S. and Selokar, A. D., Structural evolution of the Kangra recess, Himachal Himalaya: a model based on magnetic and petrofabric strains. *J. Asian Earth Sci.*, 2004, **24**, 245–258.
62. International Seismological Centre, United Kingdom, 2011; on-line bulletin; http://www.isc.ac.uk, Thatcham.
63. http://earthquake.usgs.gov/earthquakes/eqinthenews/2011/usc0005wg6/neic_c0005wg6_cmt.php

ACKNOWLEDGEMENTS. This work was funded by various grants from the Department of Science and Technology, Government of India, ARiEES, Five-Year plan grant of CSIR, to M.M., S.J. and A.M. K.A. thanks CSIR, New Delhi for JRF. We thank A. P. Krishna and his team for setting up and maintaining the Panthang permanent station and help in field measurements. M. B. Ananda, Dileep Kumar and Anjan Bhattacharyya helped with the collection of data during the early GPS measurements in Darjiling–Sikkim Himalaya. Vinee Srivastava drafted all the figures. T. S. Shrungeshwar provided technical help. Critical reviews by O. P. Mishra and an anonymous reviewer helped improve the manuscript.